

Ile115Leu mutation in the SRS1 region of an insect cytochrome P450 (CYP6B1) compromises substrate turnover via changes in a predicted product release channel

Zhimou Wen¹, Jerome Baudry², May R. Berenbaum³ and Mary A. Schuler^{1,4}

¹Department of Cell and Structural Biology, ²School of Chemical Sciences and ³Department of Entomology, University of Illinois, Urbana, IL 61801, USA

⁴To whom correspondence should be addressed.
E-mail: maryschu@uiuc.edu

CYP6B1 represents the principal cytochrome P450 monooxygenase responsible for metabolizing furanocoumarins in *Papilio polyxenes*, an insect that specializes on host plants containing these toxins. Investigations of the amino acids responsible for the efficient metabolism of these plant toxins has identified Ile115 as one that modulates the rate of furanocoumarin metabolism even though it is predicted to be positioned at the edge of the heme plane and outside substrate contact regions. In contrast to previous expression studies conducted under conditions of limiting P450 reductase showing that the Ile115-to-Leu replacement enhances turnover of xanthotoxin and other furanocoumarins, studies conducted at high P450 reductase indicate that the Ile115-to-Leu replacement reduces turnover of these substrates. Further analysis of substrate binding affinities, heme spin state and NADPH consumption rates indicate that, whereas the I115L replacement mutant displays higher substrate affinity and heme spin state than the wild-type CYP6B1 protein, it utilizes NADPH more slowly than the wild-type CYP6B1 protein at high P450 reductase levels. Molecular models developed for the wild-type CYP6B1 and mutant protein suggest that more constricted channels extending from the catalytic site in the I115L mutant to the P450 surface limit the rate of product release from this mutant catalytic site under conditions not limited by the rate of electron transfer from NADPH.

Keywords: cytochrome P450 monooxygenases/insect metabolism of toxins/molecular modeling/site-directed mutagenesis/substrate recognition sites

Introduction

Cytochrome P450 monooxygenases (P450s) are critical enzymes involved in the metabolism of a wide variety of endogenous and exogenous compounds (Schuler, 1996; Feyereisen, 1999; Omiecinski *et al.*, 1999; Scott and Wen, 2001; Danielson, 2002). The existence of multiple isoforms within individual organisms and also the broad and overlapping substrate specificities of some isoforms make functional characterization of individual P450s important for understanding biochemical pathway fluxes. The large number of P450 gene sequences that are now available indicate that P450 sequences have proliferated from a common ancestor via repeated duplication events (Nelson, 1999). As a result of subsequent diversification in the primary sequence, individual P450s share

varying degrees of amino acid identity that dictate the range of substrates metabolized. Because substrate recognition is specified not by the overall sequence but rather by a few restricted regions of the P450 structure termed substrate recognition sites (SRS) (Gotoh, 1992), it is not surprising to find P450s moderately and strongly conserved in their overall sequence displaying dramatic differences in their substrate profiles and weakly conserved P450s displaying similarities in substrate profiles. As examples, the rabbit CYP2B4 and CYP2B5 proteins contain only 12 amino acid differences, yet they differ greatly in their substrate specificities and inactivation profiles, with androstenedione hydroxylated at the 16 β -position by CYP2B4 and at the 16 α - and 15 α -positions by CYP2B5 (Kedzie *et al.*, 1991), benzyloxyresorufin *O*-debenzylated 160-fold more efficiently by CYP2B4 than by CYP2B5 (Grimm *et al.*, 1994) and 2-ethylnaphthalene selectively inactivating CYP2B4 but not CYP2B5 (Strobel *et al.*, 1999). There also exist examples of divergent P450s within the same organism displaying significant similarity in their substrate profiles.

Because the substrate versatility of P450s has great potential in the synthesis of novel chemicals and detoxification of environmental pollutants, there is strong interest in identifying the structural components of P450s that define substrate specificity and reactivity and also the efficiency of electron transfer from their NADPH-dependent P450 reductase and NADH-dependent cytochrome *b*₅ partners. Comparisons of highly conserved mammalian P450s with different reactivities coupled with site-directed mutagenesis in many of these P450s have demonstrated that amino acids within several SRS regions are the predominant determinants of substrate selectivity (Domanski and Halpert, 2001; Lewis, 2003). Among these studies, mutagenesis within the B–C loop region of SRS1 protruding into the catalytic site has highlighted these sequences as important for substrate binding to proteins in the CYP2A (Lindberg and Negishi, 1989; Negishi *et al.*, 1996a,b), CYP2B (Szklarz *et al.*, 1995; vonWachenfeldt and Johnson, 1995; Domanski *et al.*, 1999), CYP2C subfamily (Straub *et al.*, 1993a,b, 1994; Haining *et al.*, 1999) and CYP3A (Szklarz and Halpert, 1997; Roussel *et al.*, 2000; Domanski and Halpert, 2001) subfamilies. Mutagenesis within the I-helix containing SRS4 has highlighted residue 301 in the CYP2D subfamily as potentially important for electrostatic interactions with substrates (Ellis *et al.*, 1995; Modi *et al.*, 1996) and nearby residues in the CYP3A subfamily as important for substrate metabolism (Domanski *et al.*, 1998). Mutagenesis within the SRS2, SRS5 and SRS6 regions of the CYP2B (Kedzie *et al.*, 1991; He *et al.*, 1992, 1994; Halpert and He, 1993; Luo *et al.*, 1994; Szkarz *et al.*, 1995) and CYP3A (Harlow and Halpert, 1997; He *et al.*, 1997; Wang *et al.*, 1998; Xue *et al.*, 2001) subfamilies and the SRS3 region of the CYP2D subfamily (Hosseinpour *et al.*, 2001) have identified critical amino acids in these other regions.

Although SRS regions clearly influence substrate reactivities, some studies suggest that non-SRS residues also play roles in defining substrate specificity, regioselectivity and catalytic activities for the CYP2B5 and CYP2C11 proteins (He *et al.*, 1998; Biagini *et al.*, 1999). The non-SRS residues occur in the N-terminal signal sequence, between helices E and F of CYP2C11 and at the beginning of helix C and in the F–G loop of CYP2B5. Other studies have identified a number of non-SRS residues on the CYP2B4 protein surface critical for interactions with P450 electron transfer partners (Bridges *et al.*, 1998). These surface residues exist on the proximal face of the P450 protein in positions that are predicted to interact with P450 reductase via both electrostatic and hydrophobic mechanisms (Hlavica *et al.*, 2003).

CYP6B1, the subject of this paper, is the principal enzyme responsible for the ability of *Papilio polyxenes* (black swallowtail) larvae to feed on plants containing toxic furanocoumarins (Ma *et al.*, 1994; Chen *et al.*, 2002; Baudry *et al.*, 2003; Wen *et al.*, 2003; Pan *et al.*, 2004). Comparisons of CYP6B subfamily members in a number of lepidopteran insects show that over its entire length CYP6B1 shares 88% amino acid identity with CYP6B3 from the same species, 63% identity with CYP6B4 from *Papilio glaucus* (tiger swallowtail) and 53% identity with CYP6B8 from *Helicoverpa zea* (corn earworm). Varying degrees of conservation within the SRS regions of these P450s account for their common ability to metabolize planar furanocoumarins and the more restricted ability of some to metabolize other classes of plant-derived allelochemicals (Hung *et al.*, 1997; Li *et al.*, 2003, 2004; Wen *et al.*, 2003; Pan *et al.*, 2004). Molecular modeling coupled with site-directed mutageneses and type I binding analyses have identified amino acids within the SRS regions of CYP6B1 critical for the structural integrity and substrate specificity of this P450 (Chen *et al.*, 2002; Baudry *et al.*, 2003; Pan *et al.*, 2004). A particularly interesting result from these previous studies is the fact that a conservative change from isoleucine to leucine at position 115 (I115L) within the predicted B'–C loop region (SRS1) significantly increases (3- to 4-fold) the activity of CYP6B1 toward several linear furanocoumarins even though this residue is not predicted to contact the substrate (Pan *et al.*, 2004). Type I binding analyses conducted at the time indicated that the I115L mutant had both a higher affinity for its xanthotoxin substrate and a higher proportion of high spin heme (Pan *et al.*, 2004). Conducted with wild-type and mutant P450 proteins heterologously expressed with the constitutive level of P450 reductase present in Sf9 cells, these studies suggested that both catalytic site effects might potentially contribute to the enhanced metabolic capacity of the I115 mutant protein.

The subsequent establishment of a baculovirus coexpression system for insect P450 and P450 reductase demonstrated that the catalytic capacity of wild-type CYP6B1 for linear and also angular furanocoumarins is significantly enhanced at higher P450 reductase levels (Wen *et al.*, 2003). To characterize further the underlying reasons for catalytic differences between the wild-type CYP6B1 protein and its I115L mutant, we have now analyzed the metabolic capacities of both proteins under non-limiting electron transfer conditions. These comparisons suggest that isoleucine at position 115 in the wild-type CYP6B1 protein is positioned along the path of product exit from the P450 catalytic site and that its mutation significantly limits the catalytic capacity of this protein.

Materials and methods

Chemicals

Xanthotoxin (8-methoxypsoralen), bergapten (5-methoxypsoralen), psoralen and angelicin were purchased from Indofine Chemical (Belle Mead, NJ), sphondin was obtained from Dr Art Zangerl (University of Illinois), coumarin, β -NADPH, cytochrome *c*, heat-inactivated fetal bovine serum (FBS) and hemin were supplied by Sigma (St. Louis, MO) and visnagin, khellin, flavone and α -naphthoflavone were bought from Aldrich Chemical (Milwaukee, WI). Molecular biology reagents, Sf9 insect cells, SF-900 serum-free medium, pFastBac1 expression vector and DH₁₀BAC competent cells were purchased from GibcoBRL/Life Technology (Grand Island, NY). Solvents for HPLC were obtained from Fisher Scientific (Fair Lawn, NJ).

Coexpression and enzyme preparation of CYP6B1 and I115L mutant with P450 reductase

Recombinant baculoviruses for wild-type CYP6B1, its I115L mutant and house fly cytochrome P450 reductase were constructed as described by Wen *et al.* (2003) and Pan *et al.* (2004). Wild-type CYP6B1 and I115L mutant proteins were expressed alone at a multiplicity of infection (MOI) of 2 (pfu/cell) or coexpressed with house fly P450 reductase at MOI ratios varying from 2:0.05 to 2:2 (P450:P450 reductase). Infections of Sf9 cells with recombinant baculoviruses was carried out at a cell density of 0.8×10^6 cells/ml in SF-900 serum-free medium supplemented with 8–10% FBS, 50 mg/ml streptomycin sulfate and 50 U/ml penicillin, with hemin added to a final concentration of 5 mg/ml at the time of infection. After 72 h of infection, the cells were harvested by centrifugation at 3000 g for 10 min, washed once with a half cell culture volume of 100 mM cold sodium phosphate buffer (pH 7.8) and once with a one-tenth cell culture volume of cold cell lysate buffer [100 mM sodium phosphate (pH 7.8), 1.1 mM EDTA, 0.1 mM dithiothreitol, 0.5 mM phenylmethylsulfonyl fluoride, 5 μ g/ml leupeptin, 20% glycerol]. From this step, all of the procedures were carried out on ice or at 4°C. For each wash, cells were completely resuspended and repelleted at 3000 g for 10 min. Cells were finally resuspended in a one-tenth cell culture volume of cold cell lysate buffer, sonicated twice for 30 s in 5 ml batches on ice, vortex mixed for 15 s and centrifuged at 3000 g for 10 min. When microsomes were needed, 10 ml of cell lysate (i.e. the supernatant) were cleared of cell debris by centrifuging at 10 000 g (9000 r.p.m. using a Sorvall SS34 rotor) for 30 min and the resulting supernatant was centrifuged at 100 000 g (33 000 r.p.m. using a Sorvall T-865.1 rotor) for 1 h to pellet microsomes. Each S100 pellet was resuspended in 1 ml of cell lysate buffer, transferred to a 2 ml glass–glass homogenizer and homogenized on ice. Cell lysates and microsomal preparations were used immediately or aliquoted, frozen in liquid nitrogen and stored at -80°C .

Determination of P450 content and P450 reductase activities

P450 contents in cell lysates and microsome preparations were defined as described previously (Wen *et al.*, 2003). P450 reductase activities in cell lysates and microsomal preparations were determined by measuring NADPH cytochrome *c* reductase activity as described by Guengerich (1982).

Metabolism and kinetic assays

For metabolism of potential substrates, 500 μ l duplicate reactions were set up in one dram glass vials with each reaction containing final concentrations of 0.1 μ M wild-type CYP6B1 or I115L mutant protein coexpressed with house fly P450 reductase (MOI ratio of 2:2), 0.3 mM NADPH and 100 μ M (xanthotoxin, bergapten, psoralen), 25 μ M (angelicin, sphondin) or 10 μ M (visnagin, khellin, flavone, coumarin, α -naphthoflavone). Duplicate controls included reactions that were quenched at the beginning of each reaction with 125 μ l of 2 M HCl (zero time control used for total substrate determinations) and reactions incubated in the absence of NADPH (no NADPH control used for P450-independent activity determinations). Reactions were initiated with NADPH, incubated for 20 min at 30°C in a shaking water-bath and terminated with the addition of 125 μ l of 2 M HCl. For internal standardization of extraction and injection efficiencies, the same amount of a second compound having a different HPLC retention time from the compound under investigation was added; psoralen was used as the internal control for xanthotoxin metabolism and xanthotoxin was used as the control for the metabolism of all other compounds. Following addition of ethyl acetate to each reaction (2 ml to xanthotoxin, bergapten and psoralen reactions; 1 ml to angelicin and sphondin reactions; 400 μ l to all the other reactions), the samples were vortex mixed for 15 s and centrifuged at 2000 *g* for 10 min. The upper ethyl acetate phase was analyzed directly on a normal-phase HPLC column using an isocratic solvent containing 80% cyclohexane, 18% diethyl ether and 2% butanol. After correcting against the internal standard, the parent compound remaining in each sample was compared with the parent compound present in the zero time control following justification for P450-independent metabolism of each substrate. No significant P450-independent metabolism was detected in metabolism assays for any of the compounds tested. Enzymatic activities were expressed as nmol substrate disappearance per minute per nmol P450. All metabolic assays were replicated at least three times with cell lysates prepared from at least three independent batches of coexpressed proteins.

For kinetic analyses of xanthotoxin metabolism by wild-type CYP6B1 and I115L mutant proteins, various concentrations (1–200 μ M) of xanthotoxin were incubated with cell lysates coexpressing wild-type CYP6B1 or its I115L mutant with house fly P450 reductase at MOI ratios from 2:0 to 2:2. The conditions for reaction incubation, termination and extraction were the same as described above except that 0.04 μ M (final concentration) P450 was used for kinetic analyses of wild-type CYP6B1 and the I115L mutant coexpressed with house fly P450 reductase at an MOI ratio of 2:2; psoralen in the same concentration of xanthotoxin served as internal standard. All experiments were replicated at least three times with cell lysates prepared from at least two independent batches of baculovirus-infected cells. The maximum velocities (V_{\max}) for xanthotoxin metabolism by wild-type CYP6B1 and I115L mutant proteins were calculated by both the GraphPad Prism program (GraphPad Software, San Diego, CA) and Lineweaver–Burk analysis using the average values for at least three replicates.

Spectral binding titrations

Spectral binding titrations were performed using split cuvettes and double-beam mode on a Cary 100 spectrophotometer as

described previously (Wen *et al.*, 2003). Briefly, 1 ml of cell lysate buffer was added to the half of the reference and sample cuvettes closest to the light source and 1 ml of cell lysate containing 50 nM wild-type or I115L mutant protein expressed alone or with house fly P450 reductase (MOI ratio of 2:0.05) was added to the other half of the reference and sample cuvettes. Following a baseline correction scan from 350 to 500 nm, 0.2 μ l of 5 mM xanthotoxin in methanol was added to the cell lysate buffer in the reference cuvette and to the P450-containing cell lysate in the sample cuvette, samples were mixed and spectra were recorded over this same wavelength range. Spectra were taken at increasing concentrations of xanthotoxin until the absorbance difference between 390 and 420 nm was saturated. Binding titrations for xanthotoxin were replicated at least five times using a minimum of four batches of cell lysates. The spectral binding parameters [K_s , $\Delta A_{(390-420)\max}$] were obtained as described previously (Wen *et al.*, 2003).

NADPH consumption assay

NADPH consumption rates were analyzed according to Truan and Peterson (1998) with some modifications. Briefly, 500 μ l reaction volumes containing microsomes with 0.02 μ M wild-type or I115L mutant protein coexpressed with house fly P450 reductase (MOI ratio of 2:2) and 100 μ M xanthotoxin were equilibrated at room temperature for 5 min. Reactions were then initiated with the addition of 25 μ M NADPH and the absorbance decreases in NADPH were monitored at 340 nm using the double-beam mode on a Cary 100 spectrophotometer at room temperature until all NADPH was consumed. Control samples run in parallel included the same components without NADPH. To quantify the final amount of xanthotoxin metabolized, these reactions were incubated overnight at room temperature and xanthotoxin disappearance was determined by HPLC analysis as described above. Each NADPH experiment was replicated three times with microsomes prepared from two independent batches of microsomes prepared from Sf9 cells coexpressing P450 and P450 reductase. NADPH consumption rates were calculated using the initial linear decrease in absorbance at 340 nm.

Molecular modeling comparisons

Molecular models for the wild-type and I115L mutant proteins obtained using the MOE program (Chemical Computing Group, Montreal, Canada) were described by Baudry *et al.* (2003) and Pan *et al.* (2004). Potential channels connecting the heme moiety to the P450 surface interacting with P450 reductase were identified using the Site Finder facility within MOE as described by Li *et al.* (2004). Monte Carlo docking of the epoxidation product in the exit channel was performed using the 'dock' facility in MOE in the wild-type structure. The region investigated included the 'c3' exit channel identified in the wild-type enzyme. For the wild-type protein, the product was placed manually in the exit channel and the enzyme structure in the vicinity of the product was slowly relaxed using several steps of energy minimization with gradually reduced constraints on the backbone and side-chain atoms. Monte Carlo docking calculations of the product in the entire exit channel were run and the best low-energy binding modes were selected. Finally, the product–enzyme complexes were energy-minimized using the MMFF94s force field and a distant-dependent dielectric constant to

model solvent effects implicitly. For the mutant protein, the product was placed in the I115L model in the same location and orientation as the low-energy, optimized location identified in the wild-type CYP6B1 model. After energy minimization, interaction energies between the product and the enzyme were calculated for both the wild-type and mutant models.

Results

SRS1 sequence alignments

Previous site-directed mutagenesis in the *P. polyxenes* CYP6B1 protein identified an isoleucine-to-leucine replacement at position 115 that displayed 3- to 4-fold higher activity towards several linear furanocoumarins than wild-type protein when expressed with the endogenous P450 reductase present in Sf9 cells (Pan *et al.*, 2004). Type I binding analyses measuring the ability of substrates to displace water coordinated with the heme iron (Jefcoate, 1978) indicated that the I115L mutant bound xanthotoxin, a linear furanocoumarin, with higher affinity (K_s 3.7 μ M) than wild-type protein (K_s 14.6 μ M). Primary sequence alignments of the wild-type CYP6B1 with related P450s from other lepidopteran insects are shown in Figure 1 along with its alignment with rabbit CYP2B4 whose crystal structure has been defined (Scott *et al.*, 2003). These alignments indicate that Ile115 of CYP6B1 exists within the conserved B'-C loop of SRS1 found in several *Papilio* CYP6B proteins (Hung *et al.*, 1995, 1997) and that it aligns with Leu117 in the insecticide-metabolizing CYP6B8 from *H. zea* (Li *et al.*, 2000, 2004) and Val113 in CYP2B4 from rabbit (Gasser *et al.*, 1988). Molecular modeling predictions of the wild-type CYP6B1 catalytic site place Ile115 at a distance of 2.9 Å from the edge of the heme plane and outside the region contacting its planar furanocoumarin substrates (Pan *et al.*, 2004). In this position, the first of two propionic acid moieties in the catalytic heme is predicted to participate in a hydrogen bond network that involves the backbone of Ile115, Arg441, Arg127 and possibly the backbone of Arg124. Molecular replacement of Ile115 with Leu is predicted to disrupt this hydrogen bond network by lowering the number of direct hydrogen bonds between the propionic acid and surrounding residues (Pan *et al.*, 2004).

Metabolic capacities of CYP6B1 and its I115L mutant

Realizing that the activity of wild-type CYP6B1 towards xanthotoxin increased 30-fold when coexpressed with house fly P450 reductase at an MOI ratio of 2:2 (P450:P450 reductase) (Wen *et al.*, 2003), we reasoned that substrate range of CYP6B1 might be broader than previously determined at limiting P450 reductase levels. To define the range of other substrates metabolized, CYP6B1 was coexpressed with insect P450 reductase at an MOI ratio of 2:2 and monitored for

activity toward linear (xanthotoxin, bergapten, psoralen) and angular (angelicin, sphondin) furanocoumarins and also furanochromones (visnagin, khellin), flavonoid compounds (flavone, α -naphthoflavone) and unsubstituted coumarin, which are all present in the host plants of this insect. At this higher proportion of P450 reductase, wild-type CYP6B1 metabolizes linear furanocoumarins at the highest efficiencies (25.1 nmol xanthotoxin/min/nmol P450, 19.9 nmol bergapten/min/nmol P450, 16.9 nmol psoralen/min/nmol P450), angular furanocoumarins at lower efficiencies (4.5 nmol angelicin/min/nmol P450, 3.0 nmol sphondin/min/nmol P450) and furanochromones and flavonoids at substantially lower rates (Figure 2). Coumarin, modeled as an inhibitor of xanthotoxin metabolism (Baudry *et al.*, 2003), is metabolized by wild-type CYP6B1 at a negligible level.

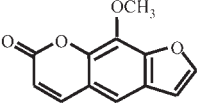
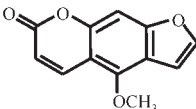
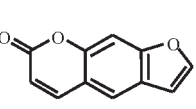
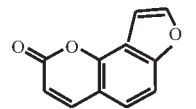
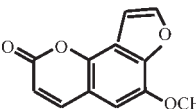
Under these same coexpression conditions, the I115L mutant metabolized linear furanocoumarins at more moderate efficiencies (10.3 nmol xanthotoxin/min/nmol P450, 8.3 nmol bergapten/min/nmol P450, 10.7 nmol psoralen/min/nmol P450) than wild-type CYP6B1, with some difference in the rankings of preferred substrates (Figure 2). The I115L mutant metabolized angular furanocoumarins at slightly lower efficiencies (3.4 nmol angelicin/min/nmol P450, 2.5 nmol sphondin/min/nmol P450) compared with wild-type CYP6B1. The I115L mutant metabolized the remaining compounds at efficiencies equivalent to wild-type CYP6B1.

Substrate specificities in P450 reductase-supplemented extracts

Compared with the high activities of wild-type CYP6B1 in P450 reductase-supplemented extracts, the disproportionately low activities of the I115L mutant towards linear and angular furanocoumarins in P450 reductase-supplemented extracts were surprising. To determine if these lower metabolic capacities resulted from variations in the kinetic parameters of these enzymes at higher P450 reductase levels, we compared the kinetic parameters of xanthotoxin metabolism by wild-type and mutant CYP6B1 proteins expressed alone with endogenous levels of P450 reductase (MOI ratio of 2:0) or coexpressed with increasing proportions of P450 reductase (MOI ratios of 2:0.05 to 2:2). As shown by Wen *et al.* (2003), at this fixed MOI of 2 for recombinant P450 virus, P450 reductase activities increase in proportion to the recombinant house fly P450 reductase virus used in the coexpression assays. When expressed without house fly P450 reductase supplementation (MOI ratio of 2:0), the maximum velocity (V_{max}) for xanthotoxin metabolism by the I115L mutant is 2-fold higher than that for xanthotoxin metabolism by wild-type CYP6B1 protein (Figure 3), in agreement with our previous analysis (Pan *et al.*, 2004). When coexpressed with increasing amounts of P450 reductase (MOI ratios decreasing to 2:2), V_{max} increases

				122	126	
rabbit	CYP2B4	GRGKIAVVDPIFQGYGVIFANGER	WR	ALR	RF	SLAT 131
				115	124	129
<i>P. polyxenes</i>	CYP6B1	DRGVEFSLDGL--GANI	FHADGDR	WR	SLRN	RF ETPLF 134
<i>P. polyxenes</i>	CYP6B3	DRGVEFSLDGL--GANI	FHADGDR	WR	SLRN	RFETPLF 134
<i>P. glaucus</i>	CYP6B4	DRGVEFSEEGE--GLNI	FHADGDR	WR	VLR	QCFTPLF 134
<i>H. zea</i>	CYP6B8	DRGVEFSKEGL--GQNL	FHADGET	WR	ALRN	RFETPIF 136

Fig. 1. Alignment of the SRS1 region of CYP6B1 with rabbit CYP2B4 and other insect CYP6B proteins using MOE alignments. Amino acid residues identical in the SRS1 region of *P. polyxenes* CYP6B1 and CYP6B3, *P. glaucus* CYP6B4, *H. zea* CYP6B8 and rabbit CYP2B4 are underlined. Arg124 and Arg129 of CYP6B1 that align with Arg122 and Arg126 of CYP2B4 are in bold. Ile115 of CYP6B1 is also in bold.

xanthotoxin		bergapten		psoralen		angelicin		sphondin	
									
WT	I115L	WT	I115L	WT	I115L	WT	I115L	WT	I115L
25.1	10.3	19.9	8.3	16.9	10.7	4.5	3.4	3.0	2.5
(0.61)	(0.36)	(0.85)	(0.83)	(0.68)	(0.14)	(0.14)	(0.66)	(0.26)	(0.17)

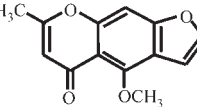
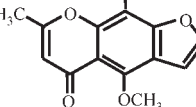
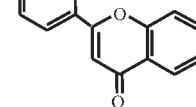
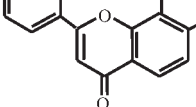
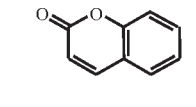
visnagin		khellin		flavone		α -naphthoflavone		coumarin	
									
WT	I115L	WT	I115L	WT	I115L	WT	I115L	WT	I115L
0.36	0.37	0.14	0.20	0.56	0.54	0.56	0.49	0.08	0.07
(0.03)	(0.05)	(0.04)	(0.05)	(0.06)	(0.06)	(0.09)	(0.07)	(0.05)	(0.01)

Fig. 2. Metabolic capacities of wild-type CYP6B1 and its I115L mutant. Wild-type CYP6B1 and the I115L mutant were coexpressed with house fly P450 reductase at an MOI ratio of 2:2 in baculovirus-infected Sf9 insect cells as described in Materials and methods. Compounds were incubated with 0.05 nmol of P450 in a 500 μ l reaction volume in the presence or absence of 0.3 mM β -NADPH. Reactions were initiated with the addition of β -NADPH and terminated after 20 min at 30°C. Substrate turnover rates were calculated on the basis of compound disappearance and are expressed in nmol substrate disappearance/min/nmol P450 derived from at least three independent protein preparations each analyzed in triplicate. Standard errors for these assays are shown in parentheses below each of the reported activities.

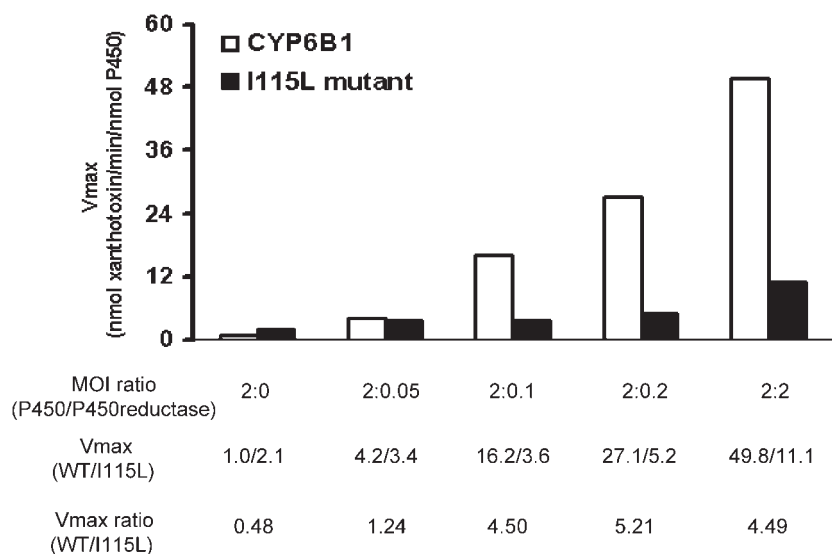


Fig. 3. Kinetic comparisons of xanthotoxin metabolism. V_{max} for the wild-type CYP6B1 and its I115L mutant coexpressed with house fly P450 reductase at different MOI ratios were determined using a Lineweaver–Burk plot and non-linear regression of the GraphPad program. No significant differences exist for these two methods. The values shown in this figure are the results obtained for non-linear regression of the GraphPad program.

49.8-fold for the wild-type CYP6B1 protein and only 5.3-fold for the I115L mutant (Figure 3). As a result, the V_{max} ratio for xanthotoxin metabolism by the wild-type vs. mutant proteins is 0.48 in the absence of coexpressed house fly P450 reductase and 1.24, 4.50, 5.21 and 4.49 at MOI ratios of 2:0.05, 2:0.1, 2:0.2 and 2:2, respectively.

Spectral binding titrations of CYP6B1 and its I115L mutant

The substantially higher V_{max} for xanthotoxin metabolism by wild-type CYP6B1 protein suggests that house fly P450

reductase interacts better with the wild-type protein than with the I115L mutant. To verify that the affinity of xanthotoxin binding to wild-type and I115L mutant proteins is unperturbed by coexpression of house fly P450 reductase, type I binding titrations were performed with these proteins in the absence and presence of P450 reductase supplementation (MOI ratio of 2:0.5) (Figure 4A). Within the standard deviations of these measurements, the binding affinities of the wild-type CYP6B1 and I115L mutant proteins for xanthotoxin are independent of the level of house fly P450 reductase expressed

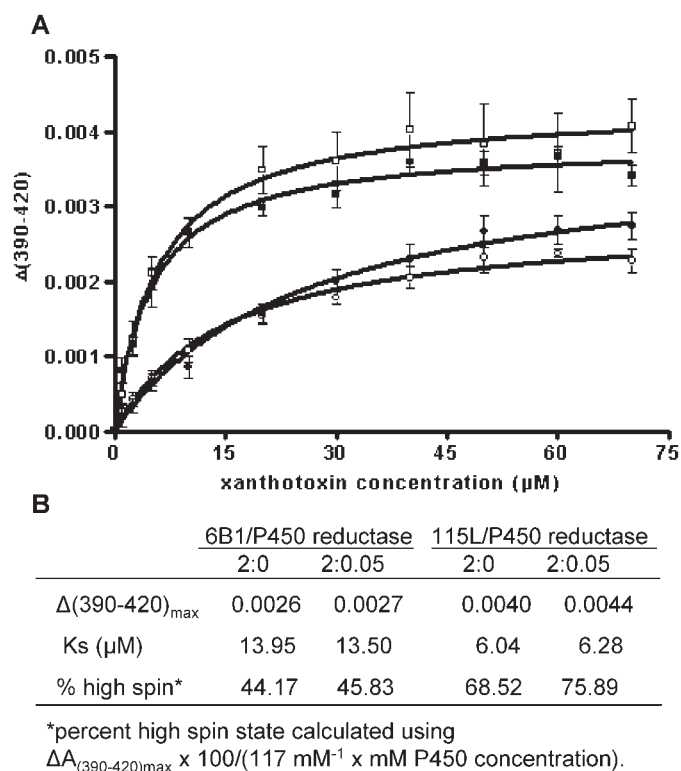


Fig. 4. Type I binding analyses for xanthotoxin. Type I binding spectra were defined using cleared cell lysates expressing the recombinant wild-type CYP6B1 and I115L mutant viruses expressed alone or coexpressed with house fly reductase (MOI ratio of 2:0.05) and various concentrations of xanthotoxin (0–70 μM). (A) Substrate binding monitored as the difference between the 390 nm maximum and 420 nm minimum is plotted in relation to the xanthotoxin concentration. (Closed circles) CYP6B1 expressed alone; (open circles) CYP6B1 expressed with house fly P450 reductase at an MOI ratio of 2:0.05; (closed squares) I115L expressed alone; (open squares) I115L expressed with house fly P450 reductase at an MOI ratio of 2:0.05. (B) Substrate binding and heme spin state parameters derived from these titration curves.

in the Sf9 cell baculovirus system (Figure 4B). When compared with the wild-type CYP6B1 protein, the binding affinity of the I115L mutant and its proportion of high spin state are substantially higher (Figure 4B). Together, these data suggest that the isoleucine-to-leucine mutation at position 115 compromises interactions of this P450 with house fly P450 reductase and/or movement of compounds between the catalytic site and surface of the protein.

Electron transfer rates for CYP6B1 and its I115L mutant

To determine if the isoleucine-to-leucine mutation affects electron transfer from NADPH, xanthotoxin-dependent NADPH consumption rates for the I115L mutant and wild-type CYP6B1 protein were monitored in microsomes derived from Sf9 cells coexpressing P450 and P450 reductase at an MOI ratio of 2:2. At this fixed amount of P450, the P450 reductase activities as determined by cytochrome *c* reduction were the same for the wild-type and mutant CYP6B1 proteins (Figure 5B), indicating that the P450:P450 reductase molar ratios are equivalent in these microsomal samples. The initial rates of NADPH consumption for each enzyme measured with 0.02 μM P450, 25 μM NADPH and 100 μM xanthotoxin (saturating substrate) indicate that wild-type CYP6B1 utilizes NADPH faster (0.38 nmol NADPH consumed/min/nmol P450)

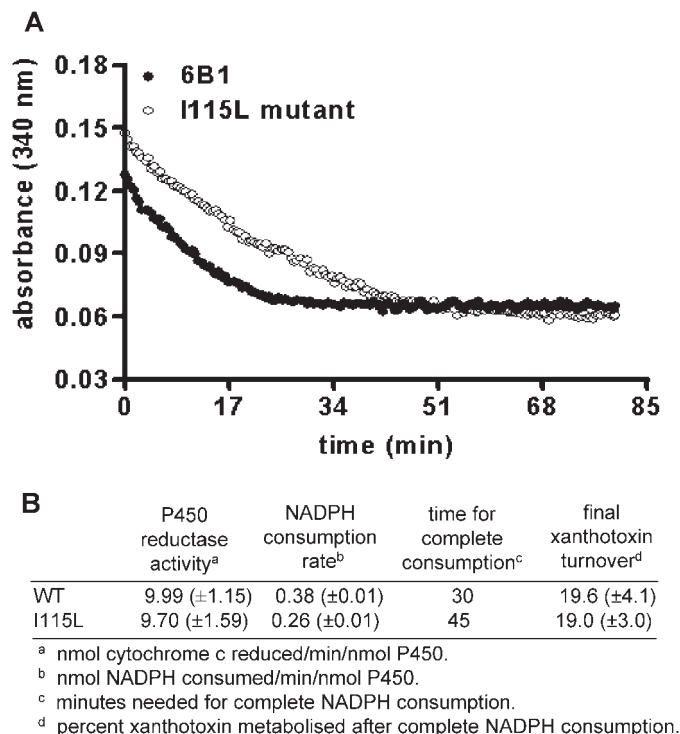


Fig. 5. NADPH consumption analysis. (A) The NADPH consumption curves in the presence of xanthotoxin for wild-type CYP6B1 and the I115L mutant proteins coexpressed with house fly P450 reductase (MOI ratio 2:2) are overlaid without adjustment for NADPH consumed by the wild-type protein in the first 20 s of the incubation. (B) Comparison of the P450 reductase activities, NADPH consumption rates and xanthotoxin metabolism for wild-type and mutant CYP6B1 proteins coexpressed with house fly P450 reductase at a fixed MOI ratio of 2:2.

than the I115L mutant (0.26 nmol NADPH consumed/min/nmol P450) (Figure 5). The slightly lower NADPH absorbance recorded at the initial time point for the wild-type CYP6B1 (Figure 5A) reflects the rapid consumption of NADPH in the time it takes to mix and begin recording absorbance profiles. Based on the plateaus for these scans, NADPH is completely consumed within 30 min by the wild-type CYP6B1 protein and within 45 min by the I115L mutant. Analysis of the amount of substrate consumed at the end of these reactions indicates that the coupling efficiencies for these two enzymes are equivalent, with comparable amounts of product formed for a given amount of NADPH (Figure 5B). These results indicate that the isoleucine-to-leucine mutation at this position compromises the rate of electron transfer between house fly P450 reductase and CYP6B1 protein without reducing the coupling efficiency between these proteins.

Structural comparisons of wild-type and mutant CYP6B1 proteins

To determine the extent to which potential surface contacts between CYP6B1 and P450 reductase might be affected by this conservative replacement, the CYP6B1 sequence was aligned with the CYP2B4 sequence whose interactions with P450 reductase and cytochrome *b*₅ have been mapped (Bridges *et al.*, 1998) and whose crystal structure has been determined (Scott *et al.*, 2003). Within the limits of aligning CYP6B1 and CYP2B4 that are only 25% identical along the length of their sequences, only two of nine surface residues involved

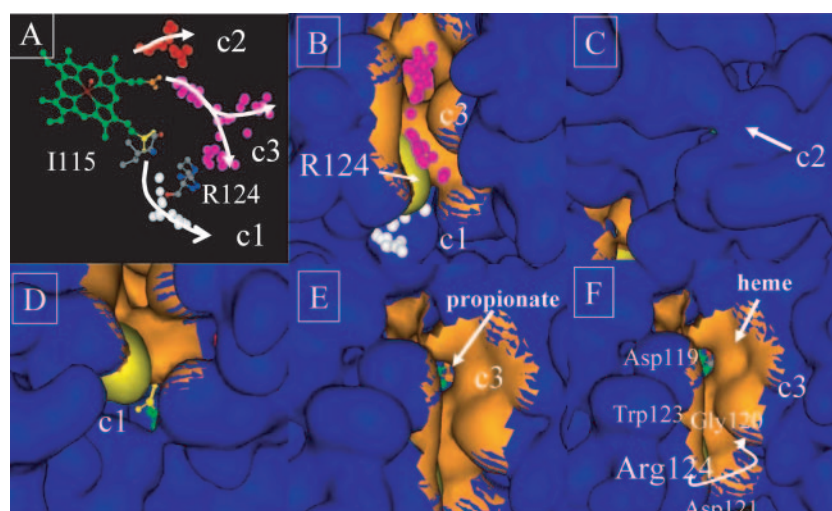


Fig. 6. Channels connecting the heme moiety to the P450–P450 reductase interaction surface in the wild-type CYP6B1 model. The heme is shown in green ball-and-stick format with its propionic acid moieties shown in yellow and orange. Potential channels in wild-type CYP6B1 are materialized using white, pink and red spheres and those connecting the heme moiety to the P450:P450 reductase interaction surface are designated as c1, c2 and c3. (A) general view of the binding site and the c1 and c3 channels passing by Arg124; (B) view of the c1 and c3 channels with the Arg124 surface shown in yellow; (C) view of the c2 channel; (D) view of the c1 channel with its channel spheres hidden and the yellow propionic acid visible; (E) view of the c3 channel with its channel spheres hidden and the orange propionic acid visible; (F) surface residues around the c3 channel.

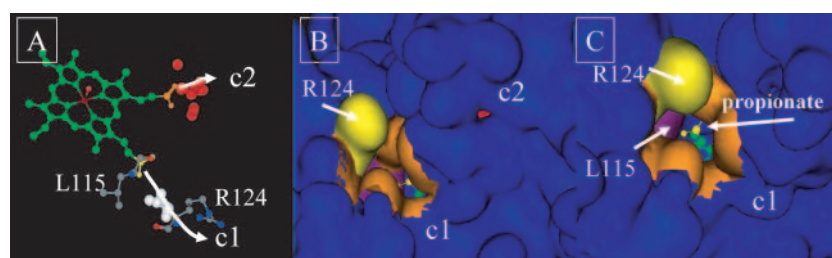


Fig. 7. Channels connecting the heme moiety to the P450–P450 reductase interaction surface in the I115L mutant. The heme is shown in green ball-and-stick format with its propionic acid moieties shown in yellow and orange. Potential channels in the I115L mutant are materialized using white and red spheres and those connecting the heme moiety to the P450–P450 reductase interaction surface are designated c1 and c2. (A) General view of the binding site and the c1 channel passing by Arg124; (B) view of the c1 and c2 channels with each channel's spheres hidden and the Arg124 and Leu115 surfaces shown in yellow and purple; (C) view of the c1 channel with yellow propionic acid visible and the Arg124 and Leu115 surfaces shown in yellow and purple.

in CYP2B4 interactions with P450 reductase (Bridges *et al.*, 1998) are absolutely conserved in primary sequence alignments with CYP6B1. Specifically, surface residues R122, R126, R133, F135, M137, K139, R422, K433 and R443 in CYP2B4 align with R124, R129, S136, K138, K140, M142, H429, P440 and K450 in the CYP6B1 primary sequence. The first two of these alignable arginines are shown in bold in the primary sequence of the C and C' helices shown in Figure 1. Highlighting of these nine amino acids in our CYP6B1 model indicates that Arg124 and Arg129 exist on the CYP6B1 surface in positions comparable to Arg122 and Arg126 on the CYP2B4 surface and that the other seven amino acids also represent surface residues with similar charge and size distributions (data not shown). Using the homology models of the predicted wild-type and I115L mutant structures described by Baudry *et al.* (2003) and Pan *et al.* (2004), the degrees of variation in these potentially interacting residues were analyzed within the superimposed structures predicted for wild-type CYP6B1 and its I115L mutant. Not surprisingly, owing to the conservative nature of the isoleucine-to-leucine replacement that occupies an internal position in this protein, relatively little difference exists in the positions of surface side chains predicted to interact with P450 reductase.

Exploring the possibility that channels connecting the heme moiety to the protein surface differ in the wild-type and mutant proteins, surface-filling models of these proteins were searched for hydrophilic and hydrophobic cavities connecting the heme to the P450 reductase interacting surface using the Alpha Site Finder facility in the MOE program. As shown in Figures 6 and 7, both the wild-type CYP6B1 and I115L mutant contain a putative channel (labeled c1 in Figures 6 and 7) extending from the surface towards one of the propionic acids of the heme moiety and a very narrow potential channel (labeled c2) that links the other propionic acid of the heme to the surface. The main difference between the models of the wild-type and I115L mutant proteins is the existence of a large potential channel in the wild-type species (labeled c3 in Figure 6) that connects the surface to the catalytic site passing by a propionic acid. This channel equivalent to the water channel described by Winn *et al.* (2002) is described for the wild-type CYP6B1 protein by Li *et al.* (2004). In the wild-type CYP6B1 protein, this channel is relatively large, ending at Arg124 (shown in yellow in Figure 6). Near its internal end, this channel connects to the catalytic site over the propionic acid on heme ring D. In the I115L mutant protein, this channel is not visible in our energy-minimized structures. Preliminary molecular dynamics

calculations on the I115L mutant indicate that the c3 channel may potentially open slightly during the course of a 100ps simulation, leading to a very narrow opening of c3 channel in the mutant as compared with the continually opened c3 channel in the wild-type protein. Together with the limited catalytic capacity of the I115L mutant, these models strongly suggest that the c3 channel serves as a conduit for product efflux from the catalytic site. Under conditions not limited in their electron transfer capacity (i.e. high P450 reductase), it can be envisioned that product efflux from the wild-type CYP6B1 catalytic site occurs efficiently through the c3 channel and product efflux from the I115L mutant is limited owing to constrictions in this channel. Longer molecular dynamics simulations are required to quantify the opening/closing dynamics of this channel in wild-type and mutant protein species. Monte Carlo docking calculations, following by energy minimization of product–enzyme complexes as described in Materials and methods, indicate that the best (lowest energy) binding mode of the epoxidation product in the wild-type c3 channel orients the C5 ring of the product toward the heme region and the C6 ring toward the surface of the enzyme. This is in agreement with the preferred binding orientation of the xanthotoxin substrate in the active site region (Baudry *et al.*, 2003). The interaction energy between xanthotoxin's epoxidation product and the enzyme is calculated to be -27.5 kcal/mol in the case of the wild-type model and -11.4 kcal/mol in the case of the mutant model. The significant difference in these predicted energies suggests that, even when the c3 channel opens in the product-containing mutant structure, the product–enzyme interaction energy in the c3 channel is substantially less favorable than in the wild-type structure.

Discussion

P450-mediated reactions represent precisely coordinated sequential steps in the process of substrate binding, electron transfer from NADPH to P450 reductase to P450, substrate oxidation and product release. Just as interference or disruption of any of these steps may reduce the reactivity of a P450 towards its substrates, facilitation of any step may enhance individual reactivities. In addition to a range of catalytic site amino acids in the CYP6B1 protein directly affecting substrate binding (Chen *et al.*, 2002; Pan *et al.*, 2004), there is now one (Ile115) whose identity clearly affects the spin state of the heme and the rate of electron transfer into the catalytic site. At the limiting levels of P450 reductase found in Sf9 cell microsomes, the conservative mutation of this residue to a leucine enhances the binding affinity of this enzyme for linear furanocoumarins and the proportion of high-spin heme resulting in substrate turnover rates that are 2-fold more efficient than the wild-type protein (Pan *et al.*, 2004). At the higher P450 reductase levels achieved in the P450:P450 reductase coexpression system tested here, the wild-type protein surpasses the furanocoumarin turnover rates of the mutant I115L protein with wild-type activities for the linear furanocoumarins xanthotoxin and bergapten being 2.4-fold higher and the angular furanocoumarin angelicin being 1.3-fold higher than that of the mutant protein. Analysis of the kinetic parameters for each of these proteins indicates that the lower activity of the I115L mutant results from slower electron transfer into the catalytic site of this protein rather than from perturbations of its substrate binding affinity or spin state.

Molecular modeling of this amino acid replacement aimed at understanding the structural role of this residue in the metabolism of plant allelochemicals suggests that some SRS1 residues critically affect substrate turnover rates because they exist on a predicted path for product efflux from the catalytic site and not because they directly contact substrate. Molecular models show that the I115L mutation has an apparent impact on the geometry of the smaller channel that potentially links the heme to the larger channel leading to the P450 surface. The I115L mutation reduces the channel's size and changes its location and/or orientation in addition to affecting the energetics of product exit. In the mutated enzyme, some of the residues that define the internal end of the larger channel vary from those defining it in the wild-type enzyme (e.g. residue 115 is involved in the I115L channel but not the wild-type channel). As a result of predicted constrictions in the path for product release from the catalytic site, the mutant enzyme displaying biochemical parameters that should contribute to increasing P450 turnover rates (high affinity for substrate, high-spin state for heme) metabolizes many substrates at lower efficiencies than wild-type CYP6B1 protein. The relatively important structural impact of the I115L mutation on the c3 channel may be due in part to the serendipity of the homology modeling process, as discussed for residues around the heme moiety (Baudry *et al.*, 2003) and the apparent 'closing' of this c3 channel in the mutant model could be due to the fact that we are considering rigid 'snapshots' of an otherwise flexible structure. However, although the docking simulations indicate that mutant 'c3-like' channel indeed opens, the thermodynamics of its product–enzyme interactions suggest that locating product in this exit channel is substantially less favorable than in the wild-type species. In the present study, the energetics of product–enzyme interactions were considered for only one point along the exit channel (corresponding to the lowest energy product location in the wild-type model). In future studies that are beyond the scope of the present work, more comprehensive investigations of the energetics and dynamics of product release can be performed using random expulsion molecular dynamics (Winn *et al.*, 2002) and/or steered molecular dynamics calculations (Isralewitz *et al.*, 2001) to determine whether thermodynamic constraints occur at other points in this predicted exit channel. Despite these limitations, the present study supports the hypothesis that the c3 channel is an avenue for product release.

More extensive analysis of the activities of these proteins toward a range of other compounds that CYP6B1 might naturally encounter in the hostplants of *P. polyxenes* has indicated that this protein is capable of metabolizing low levels of furanochromones and flavonoids. The vastly different activities of CYP6B1 toward linear furanocoumarins that are the preferred substrates and furanochromones that are marginal substrates presumably lies in the structural differences between these two categories of compounds. Probably the most significant of these structural differences is the fact that the carbonyl group at position 2 in the coumarin core structure is replaced by a methyl group at position 2 in the chromone core structure. Another is that a hydrogen at position 4 in the coumarin core structure is replaced by a carbonyl at position 4 in the chromone core structure. Substrate docking following the procedures described by Baudry *et al.* (2003) has indicated a potential binding mode for visnagin that locates the epoxidation carbon far (9.7 Å) from the iron–oxo heme intermediate (not shown)

with an energy-minimized ligand/protein interaction energy of \sim 40 kcal/mol. Even though substrate-docking calculations suggest the existence of a hydrogen bond between visnagin's 4-carbonyl and the hydroxy group of Thr372, these unfavorable interaction energies, which are significantly lower for visnagin than calculated for xanthotoxin (Baudry *et al.*, 2003), begin to explain the poor reactivity of CYP6B1 towards this substrate. Unlike the case with xanthotoxin, bergapten and other furanocoumarins, 'pulled' energy minimizations that bring the visnagin substrate within reactive distance of the heme are not energetically favored, making it both energetically and geometrically unfeasible to metabolize visnagin. The similarly low activities of CYP6B1 towards flavone and α -naphthoflavone likely result from steric constraints imposed by significantly larger benzene substituents positioned at the 2-position and the absence of a vulnerable furan ring. Clearly, metabolism of these latter compounds by *P. polyxenes* relies on other detoxification enzymes.

Acknowledgements

We thank Mr Sangeewa Rupasinghe for modeling of CYP6B1 residues potentially interacting with P450 reductase. This work was supported by NIH grants R01 GM50007 and R01 GM71826 to M.A.S.

References

- Baudry, J., Li, W., Pan, L., Berenbaum, M.R. and Schuler, M.A. (2003) *Protein Eng.*, **16**, 577–587.
- Biagini, C.P., Philpot, R.M. and Celier, C.M. (1999) *Arch. Biochem. Biophys.*, **361**, 309–314.
- Bridges, A., Gruenke, L., Chang, Y.T., Vakser, I.A., Loew, G. and Waskell, L. (1998) *J. Biol. Chem.*, **273**, 17036–17049.
- Chen, J.-S., Berenbaum, M.R. and Schuler, M.A. (2002) *Insect Mol. Biol.*, **11**, 175–186.
- Danielson, P.B. (2002) *Curr. Drug. Metab.*, **3**, 561–597.
- Domanski, T.L. and Halpert, J.R. (2001) *Curr. Drug Metab.*, **2**, 117–137.
- Domanski, T.L., Liu, J., Harlow, G.R. and Halpert, J.R. (1998) *Arch. Biochem. Biophys.*, **350**, 223–232.
- Domanski, T.L., Schultz, K.M., Roussel, F., Stevens, J.C. and Halpert, J.R. (1999) *J. Pharmacol. Exp. Ther.*, **290**, 1141–1147.
- Ellis, S.W. *et al.* (1995) *J. Biol. Chem.*, **270**, 29055–29058.
- Feyereisen, R. (1999) *Annu. Rev. Entomol.*, **44**, 507–533.
- Gasser, R., Negishi, M. and Philpot, R.M. (1988) *Mol. Pharmacol.*, **33**, 22–30.
- Gotoh, O. (1992) *J. Biol. Chem.*, **267**, 83–90.
- Grimm, S.W., Dyroff, M.C., Philpot, R.M. and Halpert, J.R. (1994) *Mol. Pharmacol.*, **46**, 1090–1099.
- Guengerich, F.R. (1982) In Hayes, A.W. (ed.), *Principles and Methods of Toxicology*. Raven Press, New York, pp. 609–634.
- Haining, R.L., Jones, J.P., Henne, K.R., Fisher, M.B., Koop, D.R., Trager, W.F. and Rettie, A.E. (1999) *Biochemistry*, **38**, 3285–3292.
- Halpert, J.R. and He, Y. (1993) *J. Biol. Chem.*, **268**, 4453–4457.
- Harlow, G.R. and Halpert, J.R. (1997) *J. Biol. Chem.*, **272**, 5396–5402.
- He, Y., Balfour, C.A., Kedzie, K.M. and Halpert, J.R. (1992) *Biochemistry*, **31**, 9220–9226.
- He, Y., Luo, Z., Klekotka, P.A., Burnett, V.L. and Halpert, J.R. (1994) *Biochemistry*, **33**, 4419–4424.
- He, Y.A., He, Y.Q., Szklarz, G.D. and Halpert, J.R. (1997) *Biochemistry*, **36**, 8831–8839.
- He, Y.Q., Harlow, G.R., Szklarz, G.D. and Halpert, J.R. (1998) *Arch. Biochem. Biophys.*, **350**, 333–339.
- Hlavica, P., Schulze, J. and Lewis, D.F.V. (2003) *J. Inorg. Biochem.*, **96**, 279–297.
- Hosseinpour, F., Hidestrand, M., Ingelman-Sundberg, M. and Wikvall, K. (2001) *Biochem. Biophys. Res. Commun.*, **288**, 1059–1063.
- Hung, C.-F., Harrison, T.L., Berenbaum, M.R. and Schuler, M.A. (1995) *Insect Mol. Biol.*, **4**, 149–160.
- Hung, C.-F., Berenbaum, M.R. and Schuler, M.A. (1997) *Insect Biochem. Mol. Biol.*, **27**, 377–385.
- Israelewitz, B., Baudry, J., Gullingsrud, J., Kosztin, D. and Schulten, K. (2001) *J. Mol. Graph. Modell.*, **19**, 13–25.
- Jefcoate, C.R. (1978) *Methods Enzymol.*, **52**, 258–279.
- Kedzie, K.M., Philpot, R.M. and Halpert, J.R. (1991) *Arch. Biochem. Biophys.*, **291**, 176–186.
- Lewis, D.F. (2003) *Arch. Biochem. Biophys.*, **409**, 32–44.
- Li, W., Schuler, M.A. and Berenbaum, M.R. (2003) *Proc. Natl Acad. Sci. USA*, **100**, 14593–14598.
- Li, X., Berenbaum, M.R. and Schuler, M.A. (2000) *Insect Biochem. Mol. Biol.*, **30**, 75–84.
- Li, X., Baudry, J., Berenbaum, M.R. and Schuler, M.A. (2004) *Proc. Natl Acad. Sci. USA*, **101**, 2939–2944.
- Lindberg, R.L.P. and Negishi, M. (1989) *Nature*, **339**, 632–634.
- Luo, Z., He, Y. and Halpert, J.R. (1994) *Arch. Biochem. Biophys.*, **309**, 52–57.
- Ma, R., Cohen, M.B., Berenbaum, M.R. and Schuler, M.A. (1994) *Arch. Biochem. Biophys.*, **310**, 332–340.
- Modi, S., Paine, M.J., Sutcliffe, M.J., Lian, L.-Y., Primrose, W.U., Wolf, C.R. and Roberts, G.C.K. (1996) *Biochemistry*, **35**, 4540–4550.
- Negishi, M., Uno, T., Darden, T.A., Sueyoshi, T. and Pedersen, L.G. (1996a) *FASEB J.*, **10**, 683–689.
- Negishi, M., Uno, T., Honkakoski, P., Sueyoshi, T., Darden, T.A. and Pedersen, L.P. (1996b) *Biochimie*, **78**, 685–694.
- Nelson, D.R. (1999) *Arch. Biochem. Biophys.*, **369**, 1–10.
- Omiecinski, C.J., Rimmel, R.P. and Hosagrahara, V.P. (1999) *Toxicol. Sci.*, **48**, 151–156.
- Pan, L., Wen, Z., Baudry, J., Berenbaum, M.R. and Schuler, M.A. (2004) *Arch. Biochem. Biophys.*, **422**, 31–41.
- Roussel, F., Khan, K.K. and Halpert, J.R. (2000) *Arch. Biochem. Biophys.*, **374**, 269–278.
- Schuler, M.A. (1996) *Crit. Rev. Plant Sci.*, **15**, 235–284.
- Scott, E.E., He, Y.A., Wester, M.R., White, M.A., Chin, C.C., Halpert, J.R., Johnson, E.F. and Stout, C.D. (2003) *Proc. Natl Acad. Sci. USA*, **100**, 13196–13201.
- Scott, J.G. and Wen, Z. (2001) *Pest. Manage. Sci.*, **57**, 958–967.
- Straub, P., Lloyd, M., Johnson, E.F. and Kemper, B. (1993a) *J. Biol. Chem.*, **268**, 21997–22003.
- Straub, P., Johnson, E.F. and Kemper, B. (1993b) *Arch. Biochem. Biophys.*, **306**, 521–527.
- Straub, P., Lloyd, M., Johnson, E.F. and Kemper, B. (1994) *Biochemistry*, **33**, 8029–8034.
- Strobel, S.M., Szklarz, G.D., He, Y.Q., Foroosh, M., Alworth, W.L., Roberts, E.S., Hollenberg, P.F. and Halpert, J.R. (1999) *J. Pharmacol. Exp. Ther.*, **290**, 445–451.
- Szklarz, G.D. and Halpert, J.R. (1997) *J. Comput.-Aided Mol. Des.*, **11**, 265–272.
- Szklarz, G.D., He, Y.A. and Halpert, J.R. (1995) *Biochemistry*, **34**, 14312–14322.
- Truan, G. and Peterson, J.A. (1998) *Arch. Biochem. Biophys.*, **349**, 53–64.
- von Wachenfeldt, C. and Johnson, E.F. (1995) In Ortiz de Montellano, P.R. (ed.), *Cytochrome P450: Structure, Mechanism and Biochemistry*, 2nd edn. Plenum Press, New York, pp. 183–223.
- Wang, H., Dick, R., Yin, H., Licad-Coles, E., Kroetz, D.L., Szklarz, G., Harlow, G., Halpert, J.R. and Correia, M.A. (1998) *Biochemistry*, **37**, 12536–12545.
- Wen, Z., Pan, L., Berenbaum, M.R. and Schuler, M.A. (2003) *Insect Biochem. Mol. Biol.*, **33**, 937–947.
- Winn, P.J., Lüdemann, S.K., Gauges, R., Lounnas, V. and Wade, R.C. (2002) *Proc. Natl Acad. Sci. USA*, **99**, 5361–5366.
- Xue, L., Wang, H.F., Wang, Q., Szklarz, G.D., Domanski, T.L., Halpert, J.R. and Correia, M.A. (2001) *Chem. Res. Toxicol.*, **14**, 483–491.

Received January 5, 2005; revised March 4, 2005;
accepted March 8, 2005

Edited by Anthony Wilkinson